Iranian Journal of Hydrogen & Fuel Cell 3(2017) 175-188

Iranian Journal of Hydrogen & Fuel Cell

IJHFC

Journal homepage://ijhfc.irost.ir

Multi-objective optimization of two hybrid power generation systems for optimum selection of SOFC reactants heat exchangers mid-temperatures

S. Sadeghi*

Department of mechanical engineering, Graduate University of advanced technology, Kerman, Iran

Article Information

Article History:

Received:
06 July 2017
Received in revised form:
27 Sep 2017
Accepted:
18 Nov 2017

Keywords

Multi-objective optimization
SOFC
Gas turbine
Steam turbine
Heat exchanger

Abstract

Increasing efficiency and decreasing cost are the main purposes in the design of power generation systems. In this study two hybrid systems, solid oxide fuel cell (SOFC)-gas turbine (GT) and SOFC-GT-steam turbine (ST), are considered. Increasing the SOFC input temperature causes thermodynamics improvement in the hybrid system operation. For this purpose, using two sets of SOFC reactant heat exchangers (primary heat exchangers and secondary heat exchangers) are recommended. Selection of the primary heat exchangers output temperature and therefore the secondary heat exchangers input temperature (heat exchangers mid-temperatures) influences the thermodynamics and economics operation of the hybrid system. This work shows that the annualized cost (ANC) and the levelized cost of energy (LCOE) act in conflict with each other. MatLab genetic optimization algorithms are used to obtain the optimum solutions. The maximum achievable efficiency is 0.599 and the minimum LCOE is 0.0163 $/kWh. Also, results show that the heat exchangers mid-temperature of air plays the main role in the operation of the hybrid system.

1. Introduction

With growing global energy consumption, decreasing fossil fuel resources, and increasing local and global environmental concerns, finding an appropriate way for efficient power generation with low emissions has become a matter of issue. Fuel cells are considered to be a suitable candidate for

*Corresponding Author's Fax: 00983433776617
E-mail address: S.Sadeghi@kgut.ac.ir

doi: 10.22104/ijhfc.2017.2376.1148

future power production owing to their high-thermal efficiency and low pollutant emissions [1]. Among the various types of fuel cells, the solid oxide fuel cell is more suitable for distributed power generation because of its high efficiency, fuel flexibility and sufficiently high operating temperature which make it a key candidate for combination with a gas turbine to produce additional electricity generation [2-6]. SOFC modeling and SOFC integrated configurations have been studied in Refs. [7-10]. In addition, a lot of researches have been carried out on modeling of hybrid SOFC-GT systems [11, 12], part load operation of SOFC-GT [13, 14], and SOFC-GT for combined heat and power generation [3].

Economic analysis can also be conducted when a power generation system is analyzed. The thermo-economic method is a suitable method for analyzing the system from both thermodynamic and economic points of view. Cheddie [15] considered a thermo-economic optimization analysis on an indirectly coupled SOFC-10 MW gas turbine hybrid system. Cheddie and Murray [16] also performed the same analysis on a SOFC-GT system with semi-direct coupling and anode recycling. Santin et al. [17] considered a thermo-economic analysis of a SOFC-GT system that uses liquid fuels. Arsalis [18] performed a thermo-economic modeling of a hybrid SOFC-GT-ST system.Thermodynamics objective functions are usually in conflict witheconomic objectives functions.

Therefore a multi-objective optimization method is used to obtain the optimum solutions. Autissier et al. [19] considered the multi-objective thermo-economic optimization of a SOFC-GT hybrid system which considered maximization of the electrical efficiency and minimization of investment cost as objectives. Palazzi et al. [20] also considered a similar study on a planar SOFC system for stationary applications. Environmental effects of power generating systems have also been taken into account in recent studies. Ahmadi and Dincer used an exergoenviromental analysis on a gas turbine power system [21] and a cogeneration gas turbine system [22]. Ahmadi et al. [23] also performed a similar analysis on a trigeneration plant.

The present study uses MatLab optimization algorithms to give the optimum thermo-economic solutions for a SOFC-GT hybrid system and a SOFC-GT-ST hybrid system. In these hybrid systems, two sets of heat exchangers are considered to heat the SOFC reactants. Using these sets of heat exchangers provide the possibility to increase the SOFC input temperature as much as desirable and so improve the performance of the hybrid systems. The optimization solutions give the optimum value for the heat exchangers mid-temperatures.

2. Mathematical modeling of the components

2.1. Solid oxide fuel cell

The fuel cell used in this study is a type of tubular solid oxide fuel cell with internal reforming [24]. For a fuel cell fed by a conventional fuel like natural gas, reforming is needed to convert the fuel into hydrogen. As reforming is done inside the cell, it is assumed that the mechanism of reactions taking place inside the cell is as follows:

Steam reforming $x \rightarrow \left[CH_4 + H_2O \rightarrow CO + 3H_2\right]$ (1)

Water gas Shifting $y \rightarrow \left[CO + H_2O \rightarrow CO_2 + H_2\right]$ (2)

Electrochemical reaction $z \rightarrow \left[H_2 + \frac{1}{2}O_2 \rightarrow H_2O\right]$ (3)

The hydrogen produced by reforming and shifting reactions with the available oxygen in the air participates in the electrochemical reaction. In the above relations x, y, and z are the molar rates of reaction progress for steam reforming, water-gas shifting, and electrochemical reactions, respectively. As the reforming and shifting reactions are in equilibrium state, the equilibrium constants of the reactions can be calculated according to equations (4-7).

$$K_{p,r} = \frac{P_{H2}^3 \times P_{CO}}{P_{CH4} \times P_{H2O}} \quad (4)$$

$$K_{p,s} = \frac{P_{CO2} \times P_{H2}}{P_{CO} \times P_{H2O}} \quad (5)$$

$$K_{p,r} = \frac{\left(\left[\dot{n}_{H2}\right]^{in} + 3x + y - z\right)^3 \times \left(\left[\dot{n}_{CO}\right]^{in} + x - y\right)}{\left(\left[\dot{n}_{CH4}\right]^{in} - x\right) \times \left(\left[\dot{n}_{H2O}\right]^{in} - x - y + z\right)} \times \frac{P_{cell}^2}{\left(\left[\dot{n}_{tot}\right]^{in} + 2x\right)^2} \quad (6)$$

$$K_{p,r} = \frac{\left(\left[\dot{n}_{CO2}\right]^{in} + y\right) \times \left(\left[\dot{n}_{H2}\right]^{in} + 3x + y - z\right)}{\left(\left[\dot{n}_{CO}\right]^{in} + x - y\right) \times \left(\left[\dot{n}_{H2O}\right]^{in} - x - y + z\right)} \quad (7)$$

The equilibrium constants of reforming and shifting reactions are directly correlated to the temperature by a polynomial equation:

$$LogK_p = AT^4 + BT^3 + CT^2 + DT + E \quad (8)$$

where *A*, *B*, *C*, *D*, and *E* are experimental constants whose values are listed by Chan [24]. The fuel utilization factor (U_f) in the anode side is defined as the ratio of reacted hydrogen to the produced hydrogen.

$$U_f = \frac{z}{3x + y} \rightarrow z = U_f \times \left(3x + y\right) \quad (9)$$

The reversible voltage of a fuel cell is calculated by the Nernst equation:

$$E = E^{\circ} + \frac{R_u T}{n_e F} Ln\left(\frac{P_{H2} P_{O2}^{0.5}}{P_{H2O}}\right) \quad (10)$$

where E^0 is the voltage of the fuel cell in standard conditions, R_u is the universal gas constant, T is the operating temperature of the fuel cell, F is the Faraday's constant, and ne is the number of circulated electron in circuit for the formation of each water molecule. The real voltage of the fuel cell is less than the Nernst voltage due to irreversibility in the fuel cell. This irreversibility can be divided into three groups of activation loss, ohmic loss, and concentration loss. The value of the real voltage is calculated according to equation (11):

$$V_{cell} = E - \left(V_{act} + V_{ohm} + V_{conc}\right) = E - \Delta V_{Loss} \quad (11)$$

The value of activation losses is equal to the sum of activation losses of the anode and cathode, and will be obtained by simplifying the Butlere-Volmers equation:

$$V_{act} = V_{act,an} + V_{act,ca} \quad (12)$$

$$V_{act} = \frac{2R_u T}{n_e F} \sinh^{-1}\left(\frac{i}{2i_{\circ,an}}\right) + \frac{2R_u T}{n_e F} \sinh^{-1}\left(\frac{i}{2i_{\circ,ca}}\right) \quad (13)$$

where i and i_0 are the current density and the exchange current density, respectively.

The ohmic losses are related to the transfer of electrons and ions in the anode, cathode, electrode, and internal connectors. The ohmic losses are obtained by equations (14-17):

$$V_{ohm} = V_{ohm,an} + V_{ohm,ca} + V_{ohm,el} + V_{ohm,inc} \quad (14)$$

$$V_{ohm} = ir \quad (15)$$

$$r = \delta\rho \quad (16)$$

$$\rho = Aexp\left(\frac{B}{T}\right) \quad (17)$$

The values of *A*, *B*, and δ in equations 16 and 17 are constant parameters that depend on the geometry and type of the fuel cell. The values of these parameters are listed by V. Akkaya [25].

The value of concentration losses is calculated by the following equations:

$$V_{conc} = V_{conc}^{an} + V_{conc}^{ca} \quad (18)$$

$$V_{conc}^{an} = \frac{R_u T}{n_e F} Ln\left(\frac{1 - i / i_{L,H2}}{1 + i / i_{L,H2O}}\right) \quad (19)$$

$$V_{conc}^{ca} = \frac{R_u T}{n_e F} Ln\left(\frac{1}{1 + i / i_{L,O2}}\right) \quad (20)$$

where i_L is the limiting current density.

The power generated by SOFC can be calculated based on the real voltage of the fuel cell by equations (21-23):

$$I_{tot} = 2Fz \tag{21}$$

$$Power_{DC-tot} = V_{cell} I_{tot} \tag{22}$$

$$Power_{AC-tot} = Power_{DC-tot} \times \eta_{inv,FC} \tag{23}$$

where I_{tot} is the total current of the fuel cell and $\eta_{invt,sofc}$ is the coefficient of inversion of direct to alternative current in the fuel cell.

Since the reforming reaction is endothermic and the shifting reaction is exothermic, the value of heat produced from the reforming and shifting reactions are obtained by:

$$\dot{Q}_r = x\left(\overline{h}_{CO} + 3\overline{h}_{H2} - \overline{h}_{CH4} - \overline{h}_{H2O}\right) \tag{24}$$

$$\dot{Q}_{sh} = x\left(\overline{h}_{CO2} + \overline{h}_{H2} - \overline{h}_{CO} - \overline{h}_{H2O}\right) \tag{25}$$

The heat produced from electrochemical reaction is supplied from two main sources. One is due to reversible reaction and the other due to the voltage losses of the fuel cell. The value of the heat produced from the electrochemical reaction also is calculated as follows:

$$\dot{Q}_{elec} = zT\Delta S - I\Delta V_{Loss} \tag{26}$$

$$\Delta S = \left(S^{\circ}_{H2O} - S^{\circ}_{H2} - \frac{1}{2}S^{\circ}_{O2}\right) + \frac{R_u}{2} Ln\left(\frac{P^2_{H2} \times P_{O2}}{P^2_{H2O}}\right) \tag{27}$$

The total net heat transfer of the solid oxide fuel cell will be obtained by the difference between the heat values of the three above equations:

$$\dot{Q}_{net} = \dot{Q}_{elec} + \dot{Q}_{sh} - \dot{Q}_r \tag{28}$$

The temperature of outflow gasses from the fuel cell can be calculated by balancing the energy, and also through the use of the trial and error method.

2.2. Compressor

Assuming an adiabatic compression process and applying Eqs. (29-31) to the system, the temperature of outlet gases and the work required for the compressor are obtained by:

$$\frac{T_{out,s}}{T_{in}} = \left(\frac{P_{out}}{P_{in}}\right)^{\frac{k-1}{k}} \tag{29}$$

$$\varsigma_{comp.} = \frac{w_{comp.,s}}{w_{comp.}} = \frac{\overline{h}_{out,s} - \overline{h}_{in}}{\overline{h}_{out} - \overline{h}_{in}} = \frac{T_{out,s} - T_{in}}{T_{out} - T_{in}} \tag{30}$$

$$\dot{W}_{comp.} = \dot{n} \times \left(\overline{h}_{out} - \overline{h}_{in}\right) \tag{31}$$

2.3. Gas turbine

By knowing the turbine inlet temperature, pressure ratio, and isentropic efficiency of the gas turbine, the value of actual work and exhaust gas temperature can be calculated according to:

$$\frac{T_{out,s}}{T_{in}} = \left(\frac{P_{out}}{P_{in}}\right)^{\frac{k-1}{k}} \tag{32}$$

$$\varsigma_{GT} = \frac{w_{GT}}{w_{GT,s}} = \frac{\overline{h}_{out} - \overline{h}_{in}}{\overline{h}_{out,s} - \overline{h}_{in}} = \frac{T_{out} - T_{in}}{T_{out,s} - T_{in}} \tag{33}$$

$$\dot{W}_{GT} = \dot{n} \times \left(\overline{h}_{out} - \overline{h}_{in}\right) \tag{34}$$

2.4. After burner

Because only a portion of inlet fuel and air are consumed in the fuel cell, the role of the after burner (AB) is to increase the system efficiency and reduce the pollution. The outlet gases of the fuel cell, which consist of steam, carbon dioxide, carbon monoxide, hydrogen, and methane in the anode side and oxygen and nitrogen in cathode side, are reacted in the after burner as follows:

$$CH_4 + 2O_2 \rightarrow 2H_2O + CO_2 \tag{35}$$

$$CO + \frac{1}{2}O_2 \rightarrow CO_2 \tag{36}$$

$$H_2 + \frac{1}{2}O_2 \rightarrow H_2O \tag{37}$$

All of the above reactions are exothermic and cause a temperature rise of outlet gases of the after burner. The temperature of outlet gases of the after burner can be calculated by the energy conservation equation and considering the efficiency of the after burner as follows:

$$\sum\left(\dot{n}\bar{h}\right)_{in} - \sum\left(\dot{n}\bar{h}\right)_{out} - \dot{Q}_{loss} = 0 \tag{38}$$

where $\dot{Q}_{loss}$ is the heat losses of the after burner, its value depending on the efficiency of the combustion.

2.5.Heat exchanger

The temperature of outlet gases from the heat exchanger is calculated based on the effectiveness-number of transfer unit method (ε_{HE} –NTU):

$$\mathring{a}_{HE} = \frac{\left(\dot{n}\bar{c}_p\right)_c\left(T_{out,c} - T_{in,c}\right)}{\left(\dot{n}\bar{c}_p\right)_{min}\left(T_{in,h} - T_{in,c}\right)} = \frac{\left(\dot{n}\bar{c}_p\right)_h\left(T_{in,h} - T_{out,h}\right)}{\left(\dot{n}\bar{c}_p\right)_{min}\left(T_{in,h} - T_{in,c}\right)} \tag{39}$$

$$\begin{aligned}\dot{Q} &= \varepsilon_{HE} \times \left(\dot{n}\bar{c}_p\right)_{min} \times \left(T_{in,h} - T_{in,c}\right) \\ &= \left(\dot{n}\bar{c}_p\right)_c\left(T_{out,c} - T_{in,c}\right) = \left(\dot{n}\bar{c}_p\right)_h\left(T_{in,h} - T_{out,h}\right)\end{aligned} \tag{40}$$

2.6. Steam turbine

The super-heater steam enters the steam turbine to generate power. The governing equations of the steam turbine are:

$$\eta_{ST} = \frac{w_{ST}}{w_{ST,s}} = \frac{\bar{h}_{out} - \bar{h}_{in}}{\bar{h}_{out,s} - \bar{h}_{in}} \tag{41}$$

$$\dot{W}_{ST} = \dot{n} \times \left(\bar{h}_{out} - \bar{h}_{in}\right) \tag{42}$$

2.7. HRSG (heat recovery steam generation)

The HRSG (heat recovery steam generation) model calculates the steam flow rate and the output steam temperature at the HRSG exit. Also, it sizes the different types of heat exchangers included in the HRSG. The energy balances on the gas and steam sides are:

$$\dot{Q}^{gas} = \dot{n}_{gas}\bar{c}_{p,gas}\left(T_{in} - T_{out}\right) \tag{43}$$

$$\dot{Q}^{steam} = \dot{n}_{steam}\bar{c}_{p,steam}\left(T_{out} - T_{in}\right) \tag{44}$$

The heat transfer rate is determined from Eq. (43), and since the gas and steam heat transfer rates are equal to each other, Eq. (44) is solved for the steam flow rate. Using simple energy balances, similar to the preceding ones, all temperatures and heat transfer rates can be calculated for all the heat exchangers. For the geometric models of the heat exchangers, the effectiveness-number of transfer unit method is used. If the heat of the exhaust gases from the gas turbine is not enough for steam generation, a super heater (SH) is used to generate the needed steam for the steam turbine.

3. Objective functions

3.1. Efficiency

Considering the total hybrid system as a control volume, the electrical efficiency and net output power are obtained by the following equations:

$$\eta_{elec} = \frac{\dot{W}_{net}}{\dot{n}_{fuel} \times LHV} \tag{45}$$

$$\dot{W}_{net} = \sum\dot{W}_{generate} - \sum\dot{W}_{consume} \tag{46}$$

3.2. Cost

In finance, the annualized cost is the cost per year of owning and operating an asset over its entire lifespan. In order to calculate ANC, annualized initial capital cost, annualized operating cost, and annualized maintenance cost will be added [26]. Since the life of different components are considered equal, replacement costs are not considered.

Annualized initial capital cost:

$$C_{acap} = C_{cap}.CRF(i,R_{proj}) \quad (47)$$

where C_{acap}, C_{cap}, CRF, i, and R_{proj} are the annualized initial capital cost, initial capital cost, capital recovery factor, real interest rate, and system lifespan, respectively.

Real interest rate:

$$i = \frac{i' - f}{f + 1} \quad (48)$$

where i' and f the nominal interest rate and inflation that are considered 0.2 and 0.15, respectively.

Capital recovery factor:

$$CFR\left(i, R_{proj}\right) = \frac{i\left(1+i\right)^{R_{proj}}}{\left(1+i\right)^{R_{proj}} - 1} \quad (49)$$

The provided equations in the Arsalis paper [18] are used to estimation the initial capital cost, maintenance cost, and operating cost of the hybrid system components.

The concept of LCOE is used to compare the cost of energy coming from different sources. The wide range of electrical power technologies available is quite varied with respect to physical principles and operation. However, the LCOE provides a common basis for comparison.

$$LCOE = \frac{ANC}{E_{AN}} \quad (50)$$

where E_{AN} is the total generated power in a year with the hybrid system.

4.Results

Fig. 1.b shows a configuration that uses GT output for heating the SOFC input reactants. In this configuration, the SOFC input temperature cannot rise to the desired value because it depends on the GT output temperature. The SOFC input temperature influences the operating temperature of the SOFC. If the SOFC input temperature increases, the operating SOFC temperature will increase. Therefore, the SOFC input temperature is an effective parameter on the operation of the SOFC and also the operation of the hybrid system. In configuration (a), SOFC reactants are heated with the GT output in the primary heat exchangers and then heated to a desired value with the after burner output in the secondary heat exchangers. The heat exchangers mid-temperatures influence the GT input temperature and also the operation of the hybrid system. In the present work, the optimum heat exchangers mid-temperatures are optimized to increase the hybrid system efficiency and decrease the hybrid system annualized cost. MatLab genetic optimization algorithms are used to obtain the optimum solutions. The variable parameters are the fuel, water, and air heat exchangers mid-temperature. First, a multi-objective optimization is used to obtain the optimum solutions with the efficiency and the annualized cost as the two objective functions. Obtaining the power generation for optimum solutions show that the LCOE acts in conflict to the annualized cost. The reason for this is that the power generation increases as the annualized cost increases. Therefore, the MatLab genetic one-objective optimization method is used to obtain the optimum solution.

4.1 Multi-objective optimization

First, the SOFC-GT hybrid system is studied. By increasing the SOFC inlet temperature, the operating temperature and voltage of the SOFC will increase. The increase in SOFC operating voltage causes an increase in the SOFC power generation resulting in an increase in the hybrid system efficiency. Table 1 shows the SOFC operating temperature and voltage for three different values of SOFC inlet temperature. If only the GT output is used to heat the SOFC reactants, the SOFC input temperature cannot rise as much as is desirable. The present work recommends that the GT output is used for the primary heating and the after burner output is used for the final heating to reach the desired SOFC input temperature. By using the after burner output for SOFC reactants heating, the GT input temperature decreases and this

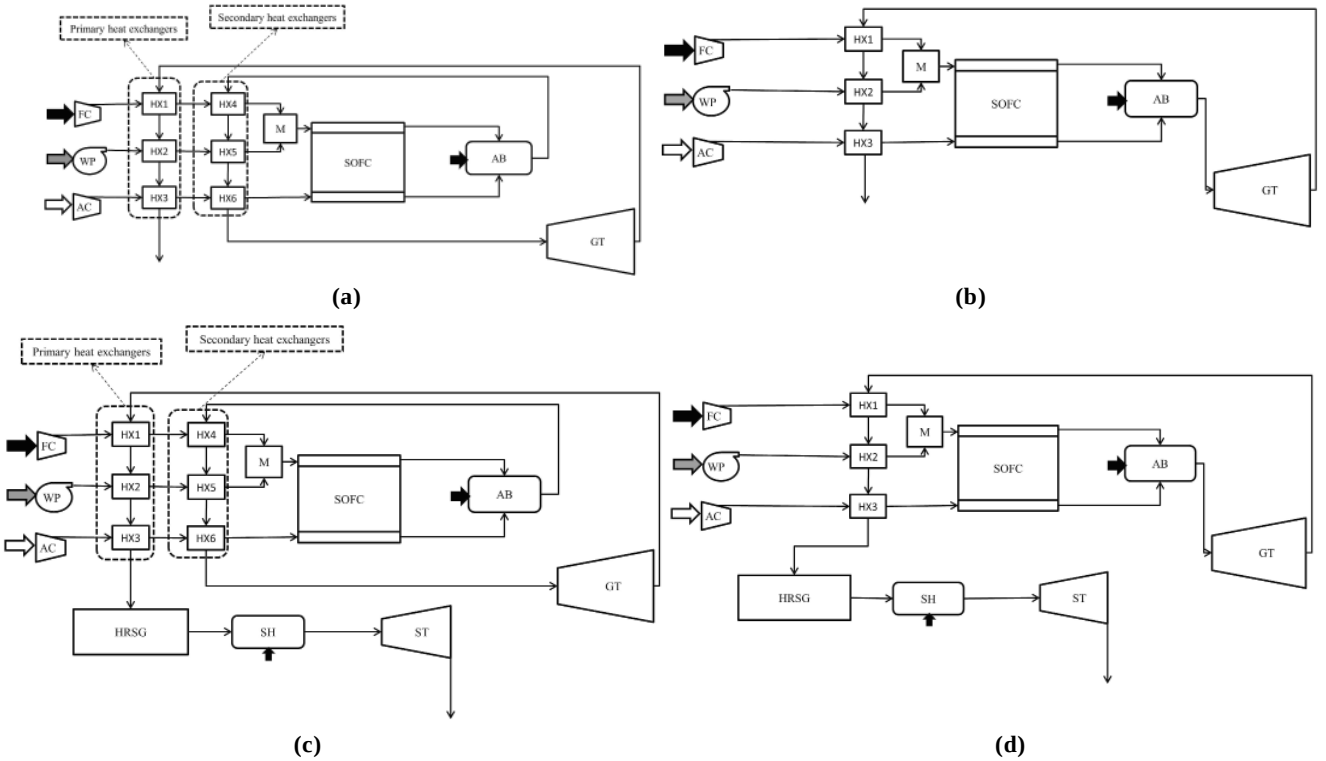

Fig.1. Different configurations of the hybrid systems, a) SOFC-GT with two sets of heat exchangers, b) SOFC-GT with a set of heat exchangers, c) SOFC-GT-ST with two sets of heat exchangers, d) SOFC-GT-ST with a set of heat exchangers

Table 1. The solid oxide fuel cell operating parameters

SOFC input temperature(K)	SOFC operating temperature(K)	SOFC operating voltage(V)	SOFC power generation(kW)
1000	1167	0.66	1143
1100	1233	0.72	1229
1150	1272	0.74	1254

Table 2. Characteristics of thermodynamics optimum solution, multi-objective optimum solution, and economic optimum solution

		Efficiency	Annualized cost ($/year)	Fuel heat exchangers mid-temperature (K)	Water heat exchangers mid-temperature (K)	Air heat exchangers mid-temperature (K)
SOFC-GT	Point A	0.583	299870	920	937	1088
	Point B	0.537	291495	999	873	831
	Point C	0.491	282857	800	700	600
SOFC-GT-ST	Point D	0.595	307890	972	856	1093
	Point E	0.561	302122	885	775	861
	Point F	0.524	294737	800	700	600

causes a decrease in the GT power generation. But the increase in the SOFC power generation due to the increscent SOFC operating temperature causes an increase in the total efficiency. Assuming the SOFC input temperature is constant, the heat exchangers mid-temperatures do not influence the SOFC operation but they do have an influence on the operation of the GT and also the hybrid system. Hence, choosing a suitable value for the heat exchangers mid-temperature is important. Whenever the heat exchangers mid-temperatures are higher, the GT input temperature and consequently the hybrid system efficiency are higher. On the other hand, whenever the heat exchangers mid-temperatures are lower, the difference in the

temperature of the hot and cold heat exchangers fluids will be suitably discharged between the primary and secondary heat exchangers. Therefore the heat exchanger surface needed and the annualized cost will decrease. Hence the change in cost and the change in efficiency with the heat exchangers mid-temperatures are in conflict with each other. To obtain the optimum heat exchangers mid-temperatures, a multi-objective optimization method must be used. In this study, the MatLab NSGAII algorithm is used for the multi-objective optimization.

Fig. 2 shows the Pareto frontier of the SOFC-GT hybrid system for three different SOFC input temperatures. It is obvious that an increase in the SOFC input temperature can generate the possibility to reach higher hybrid system efficiency. As Fig. 2 shows, the annualized cost increases with an increase in hybrid system efficiency. Three points are selected in the pareto frontier of the 1100K SOFC input temperature. Point A is the thermodynamics optimum solution. Point C is the economic optimum solution. Point B is the multi-objective optimum solution. The heat exchangers mid-temperatures of these points are shown in Table 2.

If a steam turbine is added to the SOFC-GT hybrid system, it is possible to heat the ST feed water with the primary heat exchangers output. Then the ST feed water enters to a super-heater and with the consumption of some fuel reaches the needed condition for generating power in the steam turbine. Using the ST can improve the hybrid system efficiency. The schematic of this hybrid system are shown in Fig.1c. As in the SOFC-GT hybrid system, the pareto frontier of the SOFC-GT-ST hybrid system are obtained. The pareto frontiers of the hybrid system a and c for the 1100K SOFC input temperature are compared in Fig.3. By adding the steam turbine, the efficiency and also the annualized cost will be increased. As an example, the efficiency for the thermodynamics optimum solutions increases approximately 1.5 percent and the annualized cost increases approximately 8000$/year. Fig.4 shows the pareto frontiers of the SOFC-GT-ST hybrid system for three different SOFC input temperatures. By increasing the SOFC input temperature, the efficiency and the annualized cost will also be increased. The reason for the annualized cost increment is the increase in the heat exchanger surface and the increase in the SOFC operating temperature. Three points are selected in the pareto frontier of the 1100K SOFC input temperature. Point D, E, and F are the thermodynamics optimum solution, multi-objective optimum solution, and the economic optimum solution, respectively. The heat exchangers mid-temperatures of these points are shown in Table 2.

The thermodynamics optimum solution of the hybrid system with six heat exchangers (six-HXs system) is compared with the hybrid system with three heat exchangers (three-HXs system) in Table 3. Results show that while the SOFC input temperature (1000K) is the same for the six-HXs system and three-HXs system, the three-HXs system produces higher efficiency and lower annualized cost. But the efficiency difference and the annualized cost difference are very small. In the six-HXs system, the hot and cold fluid temperature difference is greater and therefore the heat exchanger surface decreases. This surface area reduction partly compensates for the cost of the three additional heat exchangers. In ordaer to better understand the operation of the six-HXs system; the total power, the power generation of the hybrid system components, GT input and output temperature, the ST HRSG input temperature, and the heat exchangers mid-temperatures of the SOFC-GT-ST hybrid system (system c) are shown in Figs. 5, 6 and 7 for the solutions of the 1100K SOFC input temperature Pareto frontier.

Table 3. Efficiency and annualized cost of a three-HXs system and a six-HXs system for 1000K SOFC input temperature

		Efficiency	Annualized cost ($/year)
SOFC-GT	Three-HXs system	0.548	280193
	Six-HXs system	0.543	280584
SOFC-GT-ST	Three-HXs system	0.569	289937
	Six-HXs system	0.566	290949

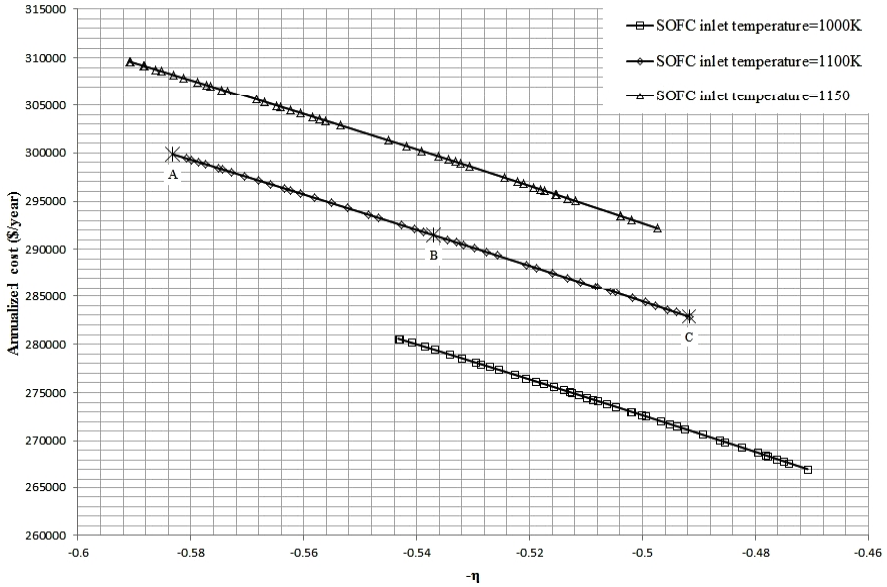

Fig.2. SOFC-GT hybrid system pareto frontier for different input SOFC temperatures.

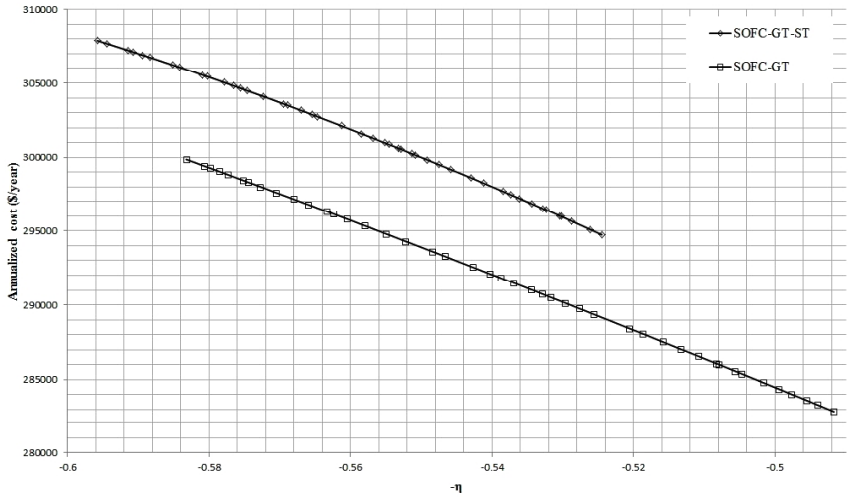

Fig.3. Pareto frontier of SOFC-GT and SOFC-GT-ST hybrid systems with six heat exchangers.

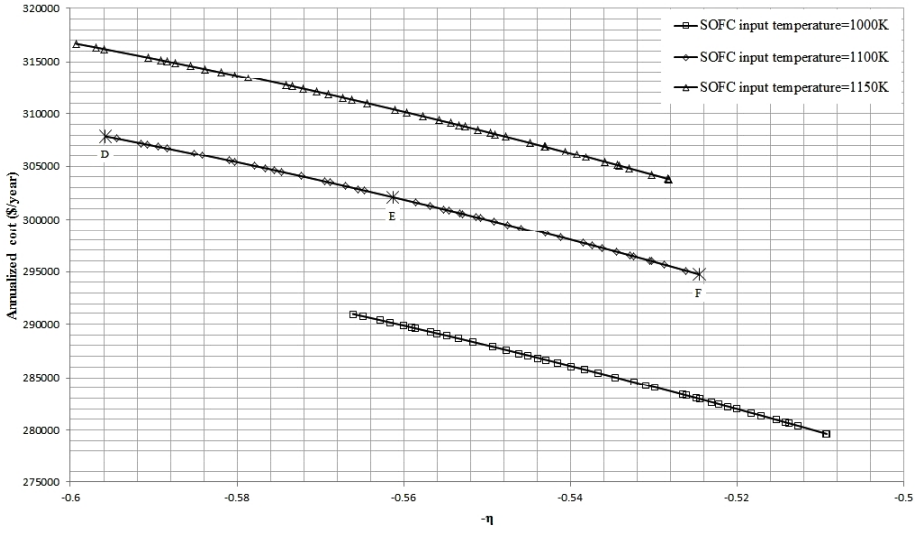

Fig. 4. SOFC-GT-ST hybrid system pareto frontier for different input SOFC temperatures.

Fig. 5 shows the total power and the power generation of the hybrid system components. Since the SOFC operation voltage is constant, the power generation of different pareto solutions are constant while the efficiency decreases. The GT power generation decreases and the ST power generation increases while the efficiency decreases. As shown in Fig. 6, the reason for the GT power reduction is the decrease in the GT input temperature. Visa versa, the ST power generation increases because the ST input temperature increases. The heat exchangers mid-temperatures are shown in Fig. 7. The heat exchangers mid-temperature of fuel and water is chosen as non-uniform between 700-1000K. The heat exchangers mid-temperature of air decreases as the efficiency decreases. Comparing the needed heat of the reactants shows that the largest portion of heat is needed for the air heating. Therefore, the heat exchangers mid-temperature of air has the main role in the operation of the hybrid system. For this reason the heat exchangers mid-temperature for fuel and water is chosen as non-uniform. With a decrease in the heat exchangers mid-temperature of air, the portion of the after burner output in the air heating increases and so the GT input temperature decreases. On the other hand, with a decrease in the heat exchangers mid-temperature of air, the portion of the GT output in the air heating decreases and so the ST input temperature increases.

4.2 One-objective optimization

The power of the SOFC-GT-ST hybrid system and the SOFC-GT hybrid system are obtained for the multi-objective method optimum solutions when the input SOFC reactants temperature is 1100K. Results, as shown in Fig. 8, show that the hybrid system power increases while the efficiency increases. Therefore, it is expected that the LCOE decreases as the efficiency increases. LCOE of the hybrid systems are calculated for the multi-objective method optimum solutions when the input SOFC reactants temperature is 1100K and are shown in Fig. 9. It is obvious that LCOE decreases as the hybrid system efficiency increases. Changes of LCOE with efficiency for different SOFC input temperatures are shown in Fig. 10. It is obvious that increasing the SOFC input temperature causes an increase in the efficiency and also in the LCOE. According to these results, for a constant SOFC input temperature, the hybrid systems can operate with a set of heat exchangers mid-temperatures that allow the hybrid systems to reach high efficiency and low LCOE. The MatLab genetic one-objective optimization method is used to obtain an optimum solution. Results are shown in Table 4 for different SOFC input temperatures. Although the ANC of the SOFC-GT-ST hybrid system is higher than the ANC of the SOFC-GT hybrid system, the LCOE of the SOFC-GT-ST hybrid system is lower than the

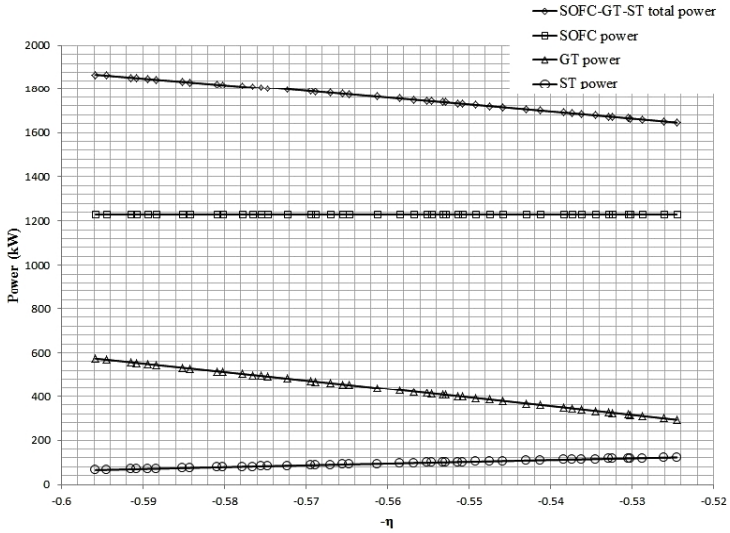

Fig. 5. Power of the hybrid system and its components for the pareto solutions of configuration c.

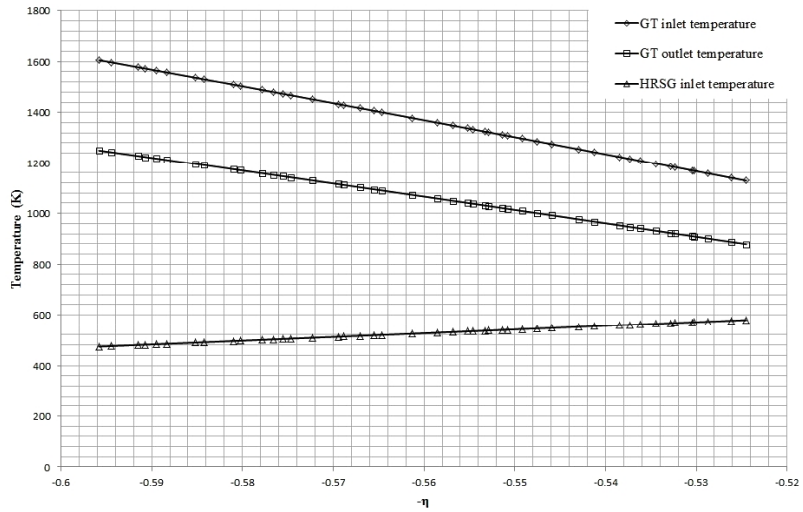

Fig. 6. GT input, GT output, and HRSG input temperatures for the pareto solutions of configuration c.

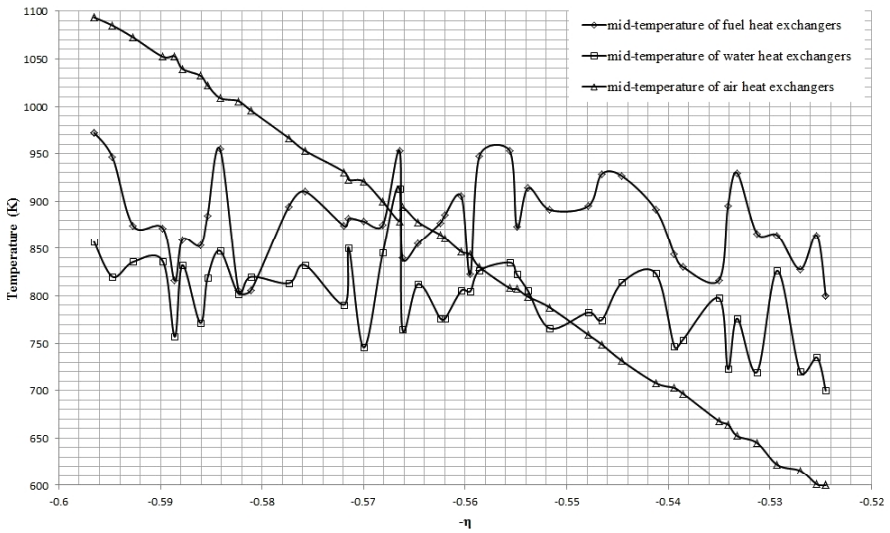

Fig.7. The heat exchangers mid-temperatures for the pareto solutions of configuration c.

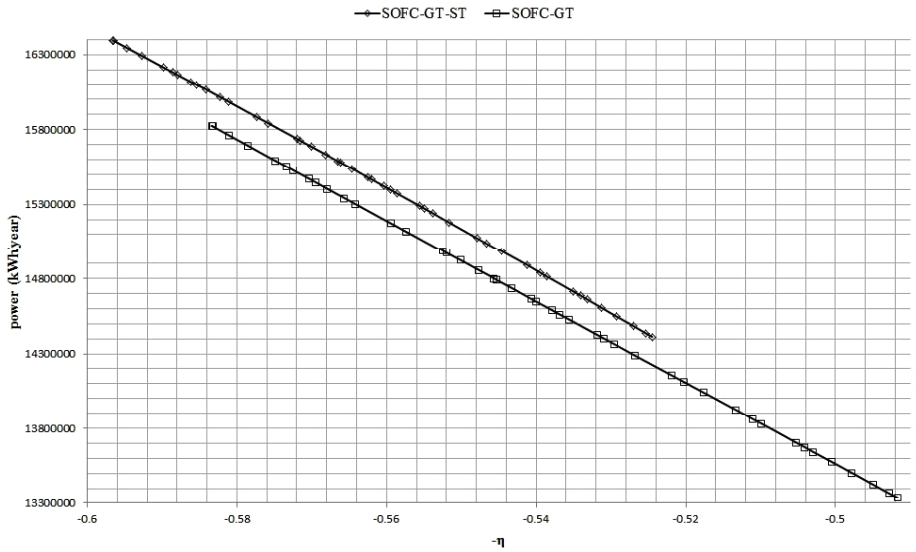

Fig. 8. Yearly power of the hybrid systems for the multi-objective method optimum solutions.

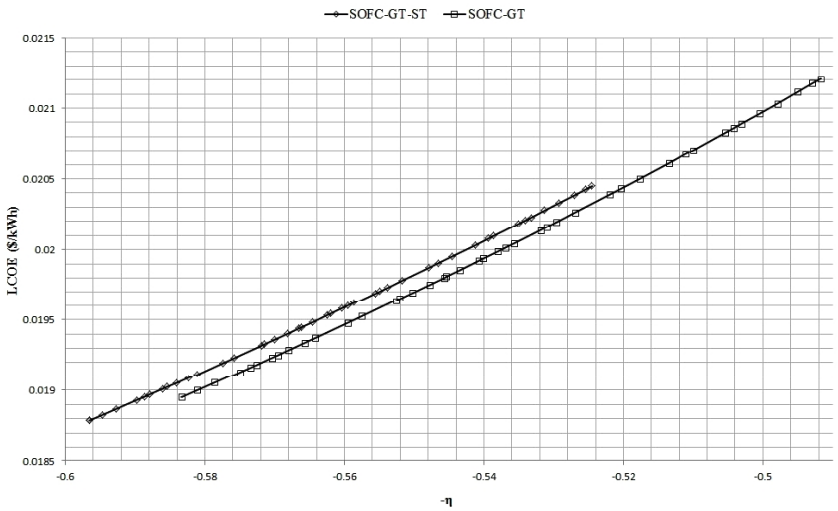

Fig. 9. LCOE of the hybrid systems for the multi-objective method optimum solutions.

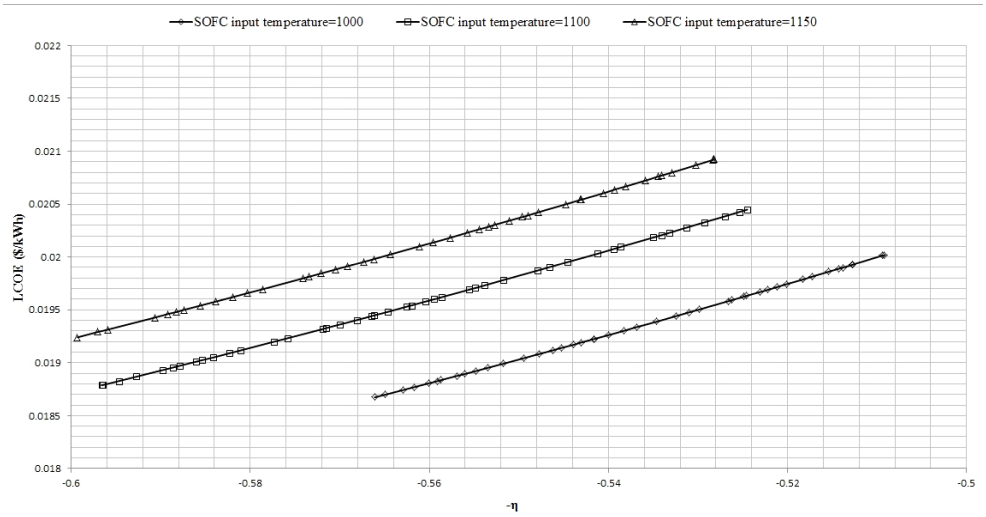

Fig. 10. LCOE of the hybrid systems for different SOFC input temperatures.

Table 4. Optimization results according to one objective (efficiency)

	SOFC input temperature (K)	Efficiency	Annualized cost ($/year)	Power Generation (kWh/year)	LCOE ($/kWh)	Fuel heat exchangers mid-temperature(K)	Water heat exchangers mid-temperature(K)	Air heat exchangers mid-temperature(K)
SOFC-GT	1000	0.543	280584	14767187	0.01901	976	769	990
	1100	0.583	299870	15723885	0.01907	920	937	1088
	1150	0.590	309630	15932997	0.0193	918	1033	1094
SOFC-GT-ST	1000	0.566	290949	15580752	0.0186	848	963	986
	1100	0.596	307999	16392890	0.0187	972	856	1063
	1150	0.599	316707	16460685	0.0192	1092	1012	1099

LCOE of the SOFC-GT hybrid system. In addition, increasing the SOFC input temperature will increase the hybrid system efficiency and also increase the LCOE because the rate of increase in the SOFC price is higher as the the SOFC input temperature increases.

5.Conclusion

In this study, two hybrid systems are considered with the goal to improve their thermodynamics and economic operation. Increasing the SOFC inlet temperature can increase the operating temperature and voltage of the SOFC and thus the hybrid system efficiency. If the GT output is used to entirely heat the SOFC reactants, the SOFC input temperature cannot rise as much as desired. Therefore, the GT output is used for primary heating and the after burner output is used for the final heating to reach the desired SOFC input temperature. Adding a steam turbine increases the hybrid system efficiency and also the annualized cost of the hybrid system. For the same SOFC input temperature, the three-HXs system produces higher efficiency and lower annualized cost, but the efficiency difference and the annualized cost difference are very small. The ANC of the hybrid systems acts in conflict with the LCOE of the hybrid systems. Because the power generation of the hybrid system will increase as the heat exchangers mid-temperature increases. Increases in the SOFC input temperature will increase the hybrid system efficiency and also increase the LCOE because the rate of increase in the SOFC price is greater as with the SOFC input temperature increases. The heat exchangers mid-temperature of air plays the main role in the operation of the hybrid system. by decreasing the heat exchangers mid-temperature of air, the portion of the after burner output in the air heating increases and the portion of the GT output in the air heating decreases; therefore, the GT input temperature decreases and the ST input temperature increases.

References

[1] Larminie J. and Dicks A., 2nd ed., Fuel cell systems explained, Academic Press, 2003.

[2] Singhal S. C. and Kendel K., 2nd ed., High temperature solid oxide fuel cell: fundamental, design and applications, Academic Press, 2003.

[3] Palsson J., Selimovic A. and Sjunnesson L., "Combined solid oxide fuel cell and gas turbine systems for efficient power and heatgeneration", J. Power Sources, 2000, 86:442.

[4] Zhang X., Chan S. H., Li G., Ho H. K., Li J. and Feng Z., "A review of integration strategies for solid oxide fuel cells", J. Power Sources, 2010, 195:685.

[5] Gupta G. K., Marda J. R., Dean A. M., Colclasure A. M., Zhu H. Y. and Kee R. J., "Performance predictions of a tubular SOFC operating on a partially reformed JP-8 surrogate", J. Power Sources, 2006, 162:553.

[6] Ni M., Leung M. K. H. and Leung D. Y. C., "A modeling study on concentration over potentials of a reversible solid oxide fuel cell", J. Power Sources, 2006, 163:460.

[7] Milewski J., Swirski K., Santarelli M. and Leone P., 1st ed., Advanced methods of solid oxide fuel cell modeling, Academic Press, 2011.

[8] Huang K. and Goodenough J. B., 1st ed., Solid oxide fuel cell technology: principles, Academic Press, 2009.

[9] Wereszczak A., Lara-Curzio E. and Bansal N. P., 1st ed., Advances in solid oxide fuel cells II, Academic Press, 2006.

[10] O'Hayre R., Cha S. W., Colella W. and Prinz F. B., 2nd ed., Fuel cell fundamentals, Academic Press, 2009.

[11] Chan S. H., Ho H. K., Tian Y., "Modeling of simple hybrid solid oxide fuel cell and gas turbine power plant", J. Power Sources, 2002, 109:111.

[12] Chan S. H., Ho H. K. and Tian Y., "Multi-level modeling of SOFC-gas turbine hybrid system", Int. J. Hydrogen Energy, 2003, 28:889.

[13] Chan S. H., Ho H. K. and Tian Y., "Modeling for part-load operation of solid oxide fuel cell-gas turbine hybrid power plant", J. Power Sources, 2003, 114:213.

[14] Costamagna P., Magistri L. and Massardo A. F., "Design and part-load performance of a hybrid system based on a solid oxide fuel cell reactor and a micro gas turbine", J. Power Sources, 2001, 96:352.

[15] Cheddie D. F., "Thermo-economic optimization of an indirectly coupled solid oxide fuel cell/gas turbine hybrid power plant", Int. J. Hydrogen Energy, 2011, 36:1702.

[16] Cheddie D. F. and Murray R., "Thermo-economic modeling of a solid oxide fuel cell/gas turbine power plant with semi-direct coupling and anode recycling", Int. J. Hydrogen Energy, 2010, 35:11208.

[17] Santin M., Traverso A., Magistri L. and Massardo A., "Thermo-economic analysis of SOFC-GT hybrid systems fed by liquid fuels", Energy, 2010, 35:1077.

[18] Arsalis A., "Thermoeconomic modeling and parametric study of hybrid SOFC-gas turbine-steam turbine power plants ranging from 1.5 to 10 MW", J. Power Sources, 2008, 181:313.

[19] Autissier N., Palazzi F., Marechal F., Van Herle J. and Favrat D., "Thermo-economic optimization of a solid oxide fuel cell, gas turbine hybrid system", J. Fuel Cell Sci. Technol., 2007, 4:123.

[20] Palazzi F., Autissier N., Marechal F. M. A. and Favrat D., "A methodology for thermo-economic modeling and optimization of solid oxide fuel cell systems", Appl. Therm. Eng., 2007, 27:2703.

[21] Ahamdi P. and Dincer I., "Thermodynamic and exergoenvironmental analyses, and multi-objective optimization of a gas turbine power plant", Appl. Therm. Eng., 2011, 31:2529.

[22] Ahamdi P. and Dincer I., "Exergoenvironmental analysis and optimization of a cogeneration plant system using multimodal genetic algorithm (MGA)", Energy, 2010, 35:5161.

[23] Ahmadi P., Rosen M. and Dincer I., "Greenhouse gas emission and exergo-environmental analyses of a trigeneration energy system", Int. J. Green Gas Control, 2011, 5:1540.

[24] Chan S. H., Low C. F. and Ding O. L., "Energy and exergy analysis of simple solid oxide fuel cell power systems", J. Power Sources, 2002, 103:188.

[25] Volkan Akkaya A., "Electrochemical Model for Performance Analysis of a Tubular SOFC", Int. J. Energy Research, 2007, 31:79.

[26] Sadeghi S . and Ameri M., "Study the Combination of Photovoltaic Panels With Different Auxiliary Systems in Grid-Connected Condition", J. Solar Energy Eng., 2014, 136:636.